JOURNAL OF MATERIALS SCIENCE 24 (1989) 2047–2056

Sinter and sinter–HIP of silicon nitride ceramics with yttria and alumina additions

I. ITURRIZA
Escuela Superior de Ingenieros Industriales, Universidad de Navarra, Calle Urdaneta 7, 20006 San Sebastián, Spain

F. CASTRO, M. FUENTES
Centro de Estudios e Investigaciones Técnicas de Guipúzcoa, Barrio de Ibaeta s/n .Apdo. 1555, 20080 San Sebastián, Spain

The sintering behaviour of silicon nitride ceramics has been investigated by preparing powder mixtures containing controlled amounts of yttria and alumina. The fired density of the compacts, having a fixed quantity of yttria, has been observed to increase with increasing amounts of alumina added to the powder. There exists, however, a maximum limit to the beneficial effect of Al_2O_3, because an excess of alumina in the powder mixture does not produce a further increase in density. Sintering of green compacts, obtained by uniaxial pressing, has been carried out at various temperatures and pressures in order to determine the relationship between fired density and the processing variables. The results obtained, after subjecting a selection of specimens to different sinter–HIP cycles, clearly show that the final density is very sensitive to the applied pressure and the time at which it is applied. The range of microstructures produced by different processing routes has also been followed by electron microscopy. From the results obtained by X-ray diffractometry it is shown that the additions of yttria and alumina not only produce denser specimens than pure silicon nitride, but also promote the α–β transformation.

1. Introduction

Sintering and hot-pressing of silicon nitride with [1–4], and without [5, 6] consolidation additives, has attracted much attention because of its wide range of potential applications as a high-temperature engineering material. Ideally the consolidation of pure Si_3N_4 would lead to a light high-strength material possessing excellent high-temperature properties. Nonetheless, sintering or hot-pressing do not seem to be viable routes for attaining fully dense pure silicon nitride except when extremely high pressures (in the order of gigapascals) are used [6]. This is due to the low self-diffusivity of this covalent material and its tendency to decompose at the sintering temperature [7].

Silicon nitride, therefore, does not sinter readily to high density without the use of additives able to form a liquid phase at the sintering temperature, so enhancing the rate of material transfer and consequently the densification rate. The kinetics of densification during hot-pressing and pressureless sintering has been interpreted [8] in terms of Kingery's model [9] of liquid-phase sintering, and the contribution of the successive stages was observed to vary with the amount and type of additive. Among the various sintering additives investigated [1, 4, 10, 11], the use of Y_2O_3 seems to be favoured because it aids the formation of a liquid which produces, on solidification, a more refractory intergranular phase than those formed by most oxide additions [8]. Nevertheless, the sinterability of this system is low [12, 13] and therefore requires the use of higher temperatures or/and the simultaneous addition of Al_2O_3 [6, 7]. Adding Al_2O_3 has, however, been reported [14] to have the effect of reducing the high-temperature strength, because it apparently prevents the crystallization of the grain-boundary phase.

Another important microscopical aspect is the α–β phase transformation during the consolidation of silicon nitride. It has been reported [4, 8] that the mechanism of solution–diffusion–reprecipitation which causes densification is at the same time a mechanism for the transformation. Therefore, the addition of Al_2O_3 to the Si_3N_4–Y_2O_3 system encourages the transformation by providing a less viscous liquid which allows rapid diffusion. On the other hand, it is noteworthy that apparently the α–β transformation can also take place, in a high purity Si_3N_4 powder, at temperatures as low as 1360° C where no liquid could be expected to be formed [14]. These authors further pointed out, that the phase transformation occurring at that temperature could even take place in the absence of nitrogen in the sintering atmosphere.

An additional technical interest is the search for alternative processes for the consolidation of silicon nitride-based ceramics. A process which seems to combine the most attractive features of both sintering and isostatic-pressing technologies is called hot isostatic pressing (HIP) [15, 16]. Strictly speaking, HIP refers to the consolidation of an encapsulated green

0022–2461/89 $03.00 + .12

compact by the simultaneous application of temperature and pressure. A further alternative route, however, is sinter–HIP which involves sintering of non-encapsulated green compacts up to the closed-porosity stage ($\simeq 90\%$ theoretical density) and subsequently applying a high pressure for the rest of the densification period [17]. This approach was employed in the present work for a few specimens, though the sintering stage was performed under a gas pressure of ~ 0.5 MPa.

In addition, the purpose of this research work was to investigate both the role of yttria and alumina, mixed at different ratios, in the sintering process of silicon nitride, and the influence the total amount of additives has on the microstructure of the final product. The phases present and the relative changes in composition between them have been examined by X-ray diffraction (XRD) and energy dispersive X-ray spectrometry (EDS) respectively. The grain morphology and the characteristics of the intergranular phases were observed by transmission electron microscopy (TEM).

2. Experimental procedure

The experimental powder used in the present work was commercial silicon nitride ($\sim 91\%$ α-Si_3N_4) whose chemical composition and specific surface area are given in Table I. Mixtures were obtained by adding controlled amounts of yttria ($\sim 99.9\%$ pure) and Al_2O_3 ($> 99\%$ pure) to the basic silicon nitride powder. Most of the work was carried out using mixtures obtained by adding different amounts of alumina, never exceeding the concentration in wt % Y_2O_3, to the basic mixtures of Si_3N_4 + 3 wt % Y_2O_3 and Si_3N_4 + 6 wt % Y_2O_3. A few other compositions were also prepared and are explicitly referred to in the text. The desired mixtures were prepared by milling the blended powders for 48 h, using a ball mill consisting of a polyethylene container and silicon nitride milling media. Green compacts were produced by uniaxial pressing 2.5 g powder samples taken from these mixtures. Powder compaction was carried out using a 16 mm internal diameter rigid steel die, and applying a compaction pressure of 100 MPa, which results in compacts having densities between 52 and 54% theoretical depending on composition.

Before sintering, the compacts were placed in a graphite crucible coated with boron nitride in order to protect the specimens from contamination. The specimens were then covered using a powder bed containing equal proportions of Si_3N_4 and BN. Sintering was performed at temperatures between 1700 and 1800° C in a graphite-heated furnace under nitrogen or argon atmospheres at a pressure of 0.5 MPa. The pressure was maintained constant during the whole heating cycle (from room temperature to the sintering temperature at a rate of 30° C min^{-1}), through the holding time (from 15 to 120 min) at temperature, and during cooling (at a rate of 35° C min^{-1}). Additional sets of specimens were subjected to sinter–HIP cycles of the type illustrated in Fig. 1, using an ASEA–HIP equipment (QIH-6), argon pressures between 10 and 150 MPa and sintering temperatures in the range 1700 to 1825° C.

TABLE I Composition and specific surface area of the Si_3N_4 powder used

Specific surface area, BET ($m^2 g^{-1}$)	Element (wt %)					
	Si (free)	Fe	Al	Ca	C	O
12	0.4	0.08	0.04	0.01	0.048	1.5

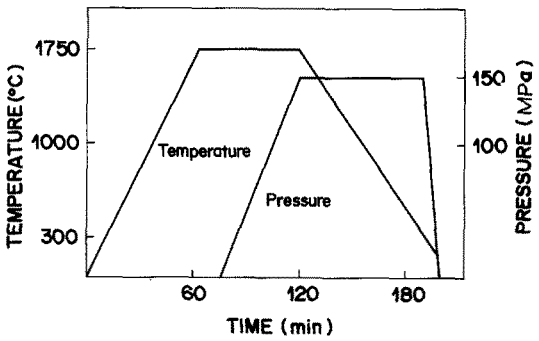

Figure 1 Schematic representation of a sinter–HIP cycle.

The characterization of the α–β phase transformation was carried out on polished samples, by X-ray diffractometry using monochromatic Cu$K\alpha$ radiation. The $\alpha:\beta$ silicon nitride ratios were calculated using a standard procedure [18] based on measurements of the ratio of intensities of the $\alpha_{20.1}$ and $\beta_{20.1}$ reflections.

For microstructural analysis in the electron microscope, discs of 3 mm diameter were obtained from bulk specimens using a diamond cutting wheel followed by a diamond coring tool. The discs were mechanically ground to about 0.2 mm, dimpled to 50 μm and ion-milled to electron transparency. A thin film of carbon was evaporated on to the foil to avoid charging during exposure to the electron beam. Analysis of thin foils was subsequently carried out using a Philips CM-12 scanning transmission electron microscope fitted with an EDAX system and a LaB_6 filament. An accelerating potential of 100 kV was invariably selected.

3. Results and discussion

The sintering behaviour of the experimental silicon nitride powder with no additives, at a sintering temperature of 1750° C and under a constant argon pressure of $\simeq 0.5$ MPa is illustrated in Fig. 2. This figure shows the dependence of three sintering parameters (final density in per cent theoretical (%TD), the weight loss in percentage (wt %) and the shrinkage ($\Delta V/V_0$))

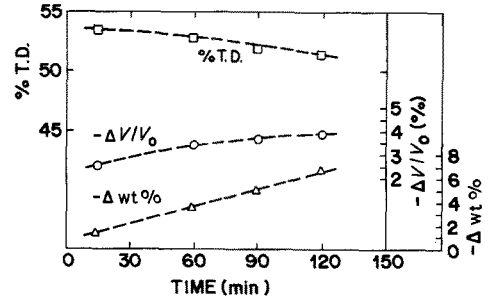

Figure 2 Variation of %TD, $-\Delta V/V_0$ and $-\Delta$ wt % on holding time at 1750° C under a constant argon pressure of 0.5 MPa for specimens of silicon nitride with no sintering aids.

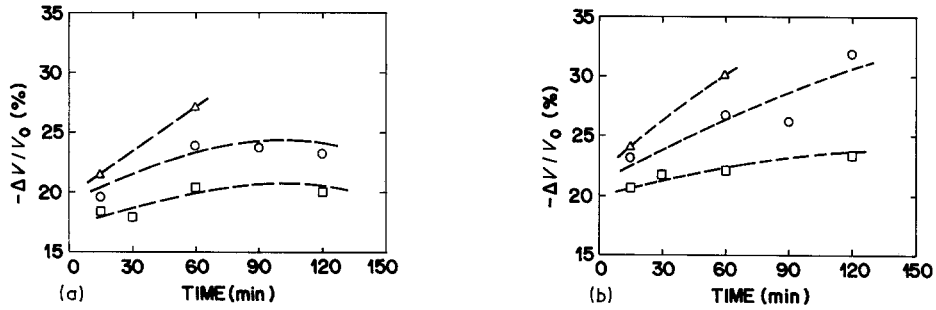

Figure 3 Dependence of shrinkage (%) on holding time and temperature for specimens sintered under a constant argon pressure for (a) Si_3N_4 + 3 wt % Y_2O_3 and (b) Si_3N_4 + 6 wt % Y_2O_3. (△) 1800° C, (○) 1750° C, (□) 1700° C.

on holding time (t) at the indicated temperature. In this case it can be observed that the density of the compacts not only does not increase, but decreases with time. This is not so unexpected, because although the shrinkage increases with time, the continued thermal decomposition of the specimens produces a decrease in weight which is, in turn, more influential on %TD than the shrinkage itself. It is noteworthy that losses up to $\simeq 7\%$ were observed (at 1700° C and after 120 min) in spite of the applied argon pressure and the use of a powder bed during sintering.

It was also noticed that increasing the sintering temperature resulted in less dense specimens due to a large weight loss. However, it must be stressed that the fractional loss in density during a fixed interval time decreased as the sintering temperature increased. This substantiates the activation, at higher temperatures, of sintering mechanisms which produce shrinkage. As a result of the competing character between the thermal decomposition of Si_3N_4 and the low diffusivity of the material, maximum densities of about 54% TD were measured, which indicates only little or no densification at all of the green body. This result is in close agreement with previously reported data [5] for pressureless sintered silicon nitride. As previously observed [4, 19, 20], adding Y_2O_3 to silicon nitride effectively aids its densification. Fig. 3 shows the result obtained in this work for 3 and 6 wt % yttria additions. It is apparent from the figure that, in general, the shrinkage of the specimens gradually increased (particularly for addition of 6 wt % Y_2O_3) as sintering progressed. Also, the figure shows a sharp increase in fractional shrinkage, for any given time interval, as temperature increases. This observation is particularly true for higher amounts of Y_2O_3 added; cf. Fig. 3b. At lower temperatures, however, little or no further shrinkage was observed after approximately 60 min. Moreover, as reported in Table II and for T = 1700° C, density seems to remain constant independent of time, although the absolute maximum reached is slightly higher as the amount of yttria added is increased.

This constancy can be understood by referring to the weight losses noted in Table II. In this case, the competing character between shrinkage and thermal decomposition compensate each other leading to a dynamic equilibrium with time. In contrast, at higher temperatures the specimen density tends to increase with time, particularly when more additive is used. This behaviour could be interpreted in terms of the amount and viscosity of the liquid phase formed at the sintering temperature. Firstly the formation of large quantities of liquid (i.e. 6 wt % Y_2O_3 as compared with 3 wt% additions) facilitates rearrangment and encourages the solution–precipitation mechanism, therefore specimens with less porosity are obtained under identical sintering conditions. Secondly, as the temperature increases, the viscosity of the liquid phase decreases, which not only produces denser specimens, but also faster densification rates.

It is also interesting to point out (see Table II) that weight losses are systematically lower, at all sintering times and temperatures, for specimens containing larger amounts of additive. This is consistent with the formation of larger quantities of liquid, because it causes a reduction of the solid–vapour interfacial area

TABLE II Measured weight losses (upper number in every square) and final densities after sintering of silicon nitride without alumina additions

	Temperature (° C)	Time (min)				
		15	30	60	90	120
Si_3N_4 + 3 wt % Y_2O_3	1700	−0.57	0.97	2.32		3.91
		67.03	65.32	66.57		65.04
	1750	0.34		3.20	5.38	6.09
		67.05		68.74	67.23	65.52
	1800	1.8		4.81		
		67.62		70.74		
Si_3N_4 + 6 wt % Y_2O_3	1700	1.39	0.78	0.00		3.21
		69.38	68.63	69.86		68.58
	1750	0.02		1.98	2.96	4.12
		70.96		72.43	71.75	76.55
	1800	1.08		2.95		
		70.75		75.74		

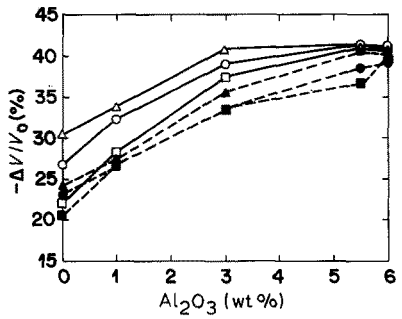

Figure 4 Influence on shrinkage of the amount of alumina added to a basic composition of Si_3N_4 + 6 wt % Y_2O_3 for specimens subjected to different sintering conditions at constant pressure. Time: (△, ○, □) 60 min, (▲, ●, ■) 15 min, at (△, ▲) 1800° C, (○, ●) 1750° C, (□, ■) 1700° C.

which reduces, in turn, the volatilization of silicon nitride. Lange [21] had also commented that weight losses are minimized when the densification kinetics is rapid.

Densification of Si_3N_4 ceramics by liquid-phase sintering has been reported [21] to involve the action of the following mechanisms: rearrangement, solution–diffusion–reprecipitation and coalescence, and the contributions of the different stages to densification are dependent on the type of additive. The influence of Al_2O_3 additions on densification is considered in Fig. 4. Adding Al_2O_3 alters the chemical composition of the liquid formed in the Si_3N_4–Y_2O_3 system alone and results in an acceleration of the densification rate. As observed in Fig. 4 the influence of Al_2O_3 concentration on densification exhibits two interesting features: materials with Al_2O_3 amounts $\geqslant 3$ wt % (particularly for $T = 1800°$ C and $t = 60$ min) show a nearly constant shrinkage of about 41% ($\simeq 92\%$ TD); and for Al_2O_3 concentrations of 6 wt % the final shrinkage is approximately the same independent of time and sintering temperature. The first point coincides with previous observations during pressureless sintering of Si_3N_4 and could be apparently interpreted [12] in terms of the formation of larger quantities of a secondary phase which has a low melting point and a low viscosity at the sintering temperature. In the present case, the second observation indicates that for high Al_2O_3 contents most of the increase in density (from green density) takes place in very short times therefore substantiating the importance of rearrangement. In addition, for a constant holding time, the almost negligible influence of temperature on densification of specimens with high Al_2O_3 contents, could indicate either a lack of SiO_2 to form liquid of lower viscosities (i.e. to enhance diffusion), or alternatively the formation of a liquid with poorer wetting characteristics (diminishing the solution stage).

The influence of additions of Al_2O_3 and Y_2O_3 at constant ratios is considered in Fig. 5. The figure shows that for a fixed alumina/yttria ratio (that is, same basic chemical composition) only the specimens with a lesser amount of liquid exhibit an almost continuous increase in density in the whole range of compositions (up to 3 wt % Al_2O_3). In contrast, the specimens containing more secondary phase (e.g. specimens with 6 wt % Y_2O_3) exhibit a maximum at a given composition (which depends on temperature, see Fig. 5b) and a subsequent decrease in density as larger amounts of Al_2O_3 are added. This will be further discussed in terms of Fig. 7.

An alternative representation of the experimental data is considered in Fig. 6 which shows the influence of the total amount of additive on densification for two different holding times. In general, it could be accepted that shrinkage increases as larger amounts of additive are used. However, a quite distinct behaviour is observed depending on whether the specimens do or do not contain a certain amount of alumina. It is interesting to observe, for instance, that a 3 : 3 composition (3 wt % Y_2O_3 + 3 wt % Al_2O_3) is more efficiently sintered than a 6 : 0 or a 6 : 3 (6 wt % Y_2O_3 and 6 wt % Y_2O_3 + 3 wt % Al_2O_3, respectively) mixture. Moreover, nearly the same density was achieved with either a 3 : 3 or a 6 : 6 mixture, which indicates that the amount and viscosity of the secondary phase formed using less additive, appears to be sufficient to produce the same volume change. It must be stressed, however, that due to weight losses, only specimens with a total amount of additive, larger or equal to $\simeq 9$ wt %, reached densities greater than 91% TD. The figure also shows that time and composition can be combined, at constant temperature, to produce a certain volume change. Additionally, the influence of sintering temperature on the densification behaviour of a material of a given composition can be appreciated by comparing Figs 6a and b.

As mentioned above, and further illustrated in Fig. 7, a maximum was observed when density data were plotted (for a constant Y_2O_3 content of 6 wt %) against the amount of Al_2O_3 added. Fig. 7 shows, tentatively, a parabolic fitting of the data points which clearly exhibits this effect. It is observed, that the height of the maximum increases slightly and its

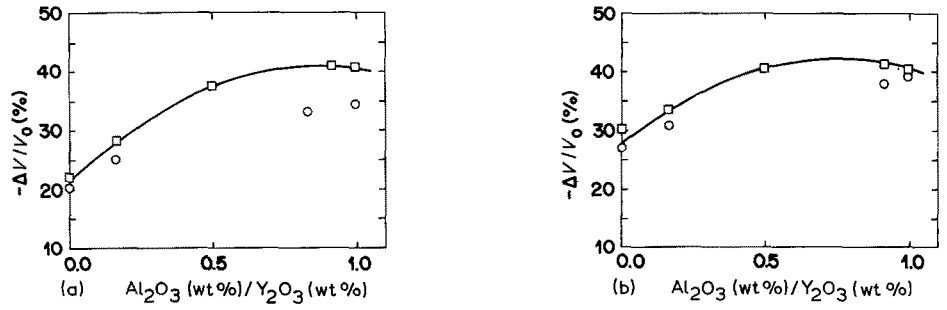

Figure 5 Variation of shrinkage (%) as a function of the Al_2O_3/Y_2O_3 ratio used in the mixture. For a sintering temperature of (a) 1700° C and (b) 1800° C; time 60 min, 5 bar argon pressure; Y_2O_3 content (○) 3 wt %, (□) 6 wt %.

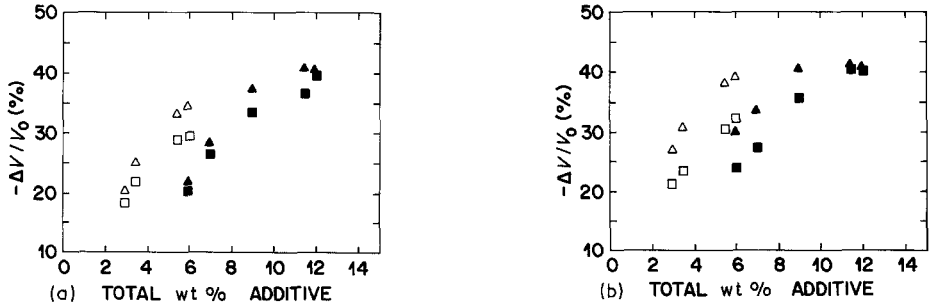

Figure 6 Per cent shrinkage as a function of the total amount of additive added. Sintering conditions are indicated in the figures (a) at 1700° C and (b) at 1800° C, at 5 bar argon pressure. Solid symbols refer to Si_3N_4 + 6 wt % Y_2O_3 specimens: holding time (△) 60 min, (□) 15 min.

position is shifted towards lower alumina concentrations, as the temperature is increased from 1750 to 1800° C under a constant argon pressure of 0.5 MPa. The appearance of such a maximum was systematically observed at all compositions and under diverse sintering conditions. For every set of conditions, therefore, an optimum alumina concentration will lead to maximum density, and any additions in excess will be reflected in larger weight losses.

The application of high pressure, as in sinter–HIP, enhances the densification process and reduces weight losses by thermal decomposition. This is clearly appreciated in Fig. 7 by comparing the curves obtained at 1750° C. The application of 50 MPa pressure during a sinter–HIP cycle resulted in an acceleration of the densification kinetics. As observed in the figure, this is a constant effect for specimens with densities below $\simeq$ 90% TD, however, a larger influence is observed for specimens with Al_2O_3 contents in excess of $\simeq$ 3 wt %. This behaviour could be attributed to two different reasons: firstly, the application of pressure enhances both rearrangement and the solution–precipitation process, and therefore an essential improvement of densification behaviour is observed at all compositions; secondly in the present case not only the thermal decomposition was suppressed but also a weight gain, probably from the powder bed, was found in all alumina-containing specimens. Additionally, the more pronounced influence of pressure on specimens having higher Al_2O_3 contents is probably also related to the fact that these specimens had a high density at the moment the pressure was applied. This would ensure application of pressure to specimens in the closed porosity stage, that is to samples impermeable to gas. Further analysis of this figure shows that equivalent results are obtained (for $Al_2O_3 \leqslant 3$ wt %) by applying 50 MPa at 1750° C or by sintering at 1800° C. Therefore, applying a pressure of 50 MPa effectively reduced the sintering temperature by 50° C approximately.

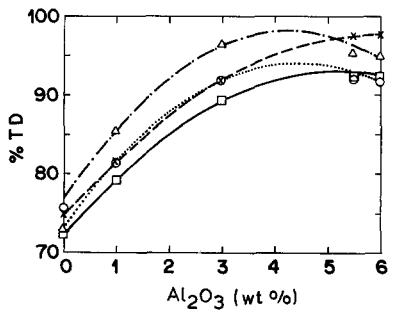

Figure 7 Influence of SiO_2 content on final density after sintering for 60 min at (×) 1750° C, 50 MPa Ar, (△) 1800° C, 5 bar N_2, (○) 1800° C, 5 bar Ar, (□) 1750° C, 5 bar Ar.

The influence of a nitrogen atmosphere during sintering was also considered. As observed in Fig. 7, the densification process follows the same trend as with argon. Using nitrogen, however, increases the densification kinetics producing a nearly constant increase in density of about 5% for all alumina concentrations. This increase is not surprising due to the high solubility of nitrogen in this ceramic system. It is also interesting to observe that the maximum density reached either using a sinter–HIP cycle with argon gas or low pressure sintering with nitrogen is approximately the same (> 98% TD), although in the latter case this is achieved advantageously for a lower alumina content.

The α–β phase transformation has been observed to be one of the characteristic features during sintering of this high α-Si_3N_4 powder with and without the use of additives. Fig. 8 shows three typical X-ray recordings corresponding to the initial powder, a partially transformed and a fully transformed sintered specimen. The figure shows the region of interest for the

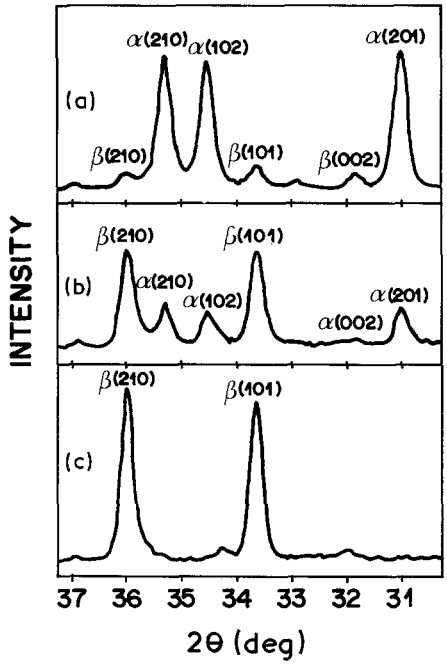

Figure 8 X-ray recordings corresponding to (a) the as-received silicon nitride powder, (b) Si_3N_4 + 6 wt % Y_2O_3 + 1 wt % Al_2O_3 after 15 min at 1700° C and 0.5 MPa Ar, (c) Si_3N_4 + 6 wt % Y_2O_3 + 1 wt % Al_2O_3 after 60 min at 1700° C and 0.5 MPa Ar.

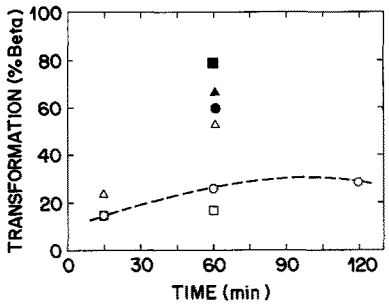

Figure 9 Amount of β-phase present in Si_3N_4 specimens during different times. Sintering conditions: (□) 1700° C, 5 bar Ar, (○) 1750° C, 5 bar Ar, (△) 1800° C, 5 bar Ar, (▲) 1750° C, 50 MPa Ar, (●) 1750° C, 150 MPa Ar, (■) 1825° C, 10 MPa Ar.

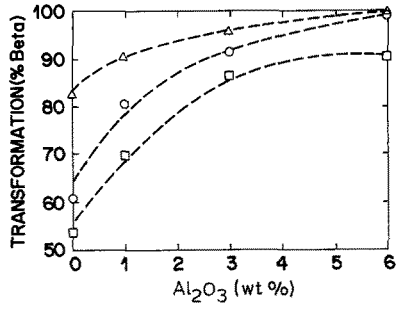

Figure 10 Effect of alumina content on the amount of β-phase present in specimens sintered at different temperatures under (△) nitrogen (5 bar) or (○, □) argon (5 bar) atmospheres: Si_3N_4 + 6 wt % Y_2O_3, 15 min; (△, ○) 1750° C, (□) 1700° C.

quantitative determination of the α/β content in every specimen. During sintering of the experimental powder without additives, the α–β transformation was observed to occur progressively with time. The results in Fig. 9, show the influence of different sintering conditions on the transformation and indicate that up to 1750° C and 120 min only less than 30% of the material had been transformed. The increase of the transformation kinetics by the application of higher temperatures and/or pressures is clearly apparent. For instance, increasing the pressure in two orders of magnitude at 1750° C (from 0.5 to 50 MPa) resulted, after a sintering time of 60 min, in an increase by a factor of three of the amount transformed. The same effect can be seen to occur by increasing the temperature in 50° C, whereas at 1750° C, a further increase in pressure (from 50 to 150 MPa) did not produce any additional transformation. This is in contrast to the observations made by Yeheskel *et al.* [22].

Fig. 10 shows, however, that fully transformed material can be obtained by the use of additions of yttria and alumina. By comparing Figs 9 and 10 it is realized that adding 6 wt % yttria (with no alumina) accelerates the transformation kinetics with respect to that of the original powder by nearly a factor of three (at 1750° C), clearly substantiating the influence of the liquid phase formed. This observation provides evidence for a solution–precipitation reaction of the form proposed by some authors [4, 22, 23]. The dependence of the percentage of β on the alumina concentration shown in Fig. 10, also seems to lend support to a solution–precipitation mechanism for the transformation. However, the possibility of a transformation in the absence of a liquid, as observed by Greskovich and Prochazka [14] cannot be ruled out. Although in the present case the transformation of Si_3N_4 without additives could also have occurred through the liquid which most probably forms, from the reaction of the SiO_2 thin film covering the particles with the impurities and the products of thermal decomposition (i.e. silicon and nitrogen). The influence of nitrogen as a sintering atmosphere can therefore be understood because it could appreciably dissolve in the silicate liquid (of the system Si_3N_4–Y_2O_3–Al_2O_3) at high temperatures, so that reaction of silicon and nitrogen and the transport of these atoms through the liquid phase would certainly accelerate the transformation kinetics.

From the data obtained it can therefore be realized that the kinetics for both densification and transformation presented many similarities and followed the same trends. That is, the factors which caused an increase in density also produced a larger transformed fraction. However, the rates at which these phenomena took place were completely different so that a substantial densification occurs after completion of the phase transformation. Even in those cases where a partial transformation was observed, densification in percentage was always more sluggish. This was the general case under all conditions of composition, temperature and pressure; and contrasts with the results reported by Shimada *et al.* [6]. In the present case, the later stages of densification, where these authors observed a correspondence between densification and transformation, occurred with no phase transformation. On the other hand, as observed by Hampshire and Jack [8], it is likely that adding yttria caused appreciable precipitation of β in the contact areas without significant material transport. This is due to the high viscosity of the liquid through which diffusion is relatively slow.

From the specimens analysed by TEM it was found that sintering of Si_3N_4 with additions of Y_2O_3 and Al_2O_3, proceeds with the formation of a microstructure which contains α and β-Si_3N_4 grains, crystalline regions rich in yttria, porosity and an amorphous

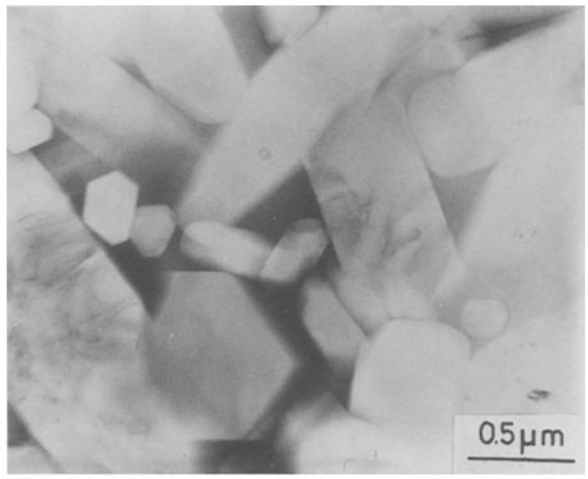

Figure 11 Transmission electron micrograph of a typical area of a specimen containing 6 wt % Y_2O_3 + 6 wt % Al_2O_3 additions and sintered at 1750° C for 60 min at a constant argon pressure at 0.5 MPa.

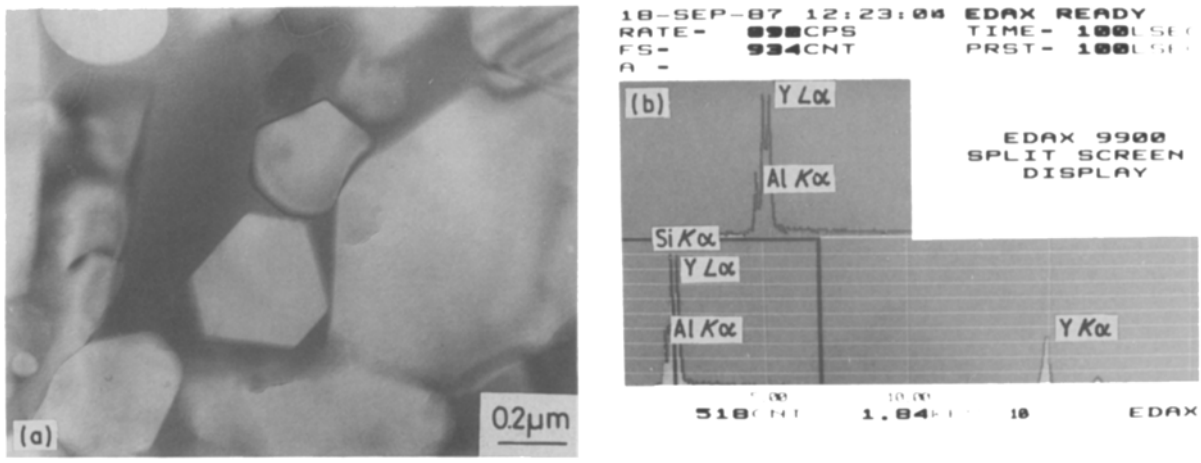

Figure 12 Intergranular glassy phase in Si_3N_4 + 6 wt % Y_2O_3 + 6 wt % Al_2O_3 sintered at 1750° C for 60 min under a constant nitrogen pressure of 0.5 MPa. (a) Relatively large area forming part of the microstructure and (b) EDS spectrum taken from the area revealed by the contamination mark.

intergranular phase depending on sintering conditions and composition. The micrograph in Fig. 11, which corresponds to a fully transformed specimen, shows the presence of typical β-grains with a mean size of approximately 1.5 μm and an average aspect ratio of about 5:1. The microstructure also contained an intergranular glassy phase (in the dark field) which strongly absorbed the incident electron beam, therefore suggesting a high yttria content. Qualitative EDS analysis (e.g. Fig. 12b) carried out on several specimens confirmed this point and revealed the presence of aluminium and silicon as additional constituents of its composition. The overall microstructure contained some large intergranular areas like that shown in Fig. 12a, but this second phase was mainly found surrounding the β-Si_3N_4 grains.

A thin ($\simeq$ 0.5 to 2 nm) film of glass was almost invariably observed, as it has also been recently reported [24], between the β grains and its presence was revealed by centred dark-field (CDF) images (e.g. Fig. 13a) which enhances the grain-boundary interphase contrast. Fig. 13b shows the diffraction pattern obtained from the glass and the position of the objective aperture to select a small part of the diffracted ring. In other parts of the microstructure much larger grains than average were found (Fig. 14) which were probably produced by an anomalous grain growth or were alternatively inherited from the Si_3N_4 starting powder (possibly through agglomeration).

Additionally, close examination of the microstructures exhibited by specimens subjected to sinter–HIP revealed some interesting differences with respect to the sintered specimens. Fig. 15 shows the typical microstructure of a specimen after a sinter–HIP cycle applying an argon pressure of 50 MPa. The microstructure still consisted of β-Si_3N_4 grains surrounded by a glassy intergranular phase which was, however, more homogeneously distributed. That is, fewer and smaller intergranular areas like the one shown in Fig. 12a, were found. In general, the morphology of the β-Si_3N_4 grains was unchanged; however, noticeable changes were observed, particularly at some β-grains contact points. These areas (arrowed in Fig. 15) revealed the presence of dislocations near the contact points indicating that they were subjected to a high stress after the α–β transformation. It is important to notice that in this condition a "penetration effect" of one grain into another was commonly observed, with the grain containing a higher dislocation density being apparently consumed by the cleaner grain. This "grain

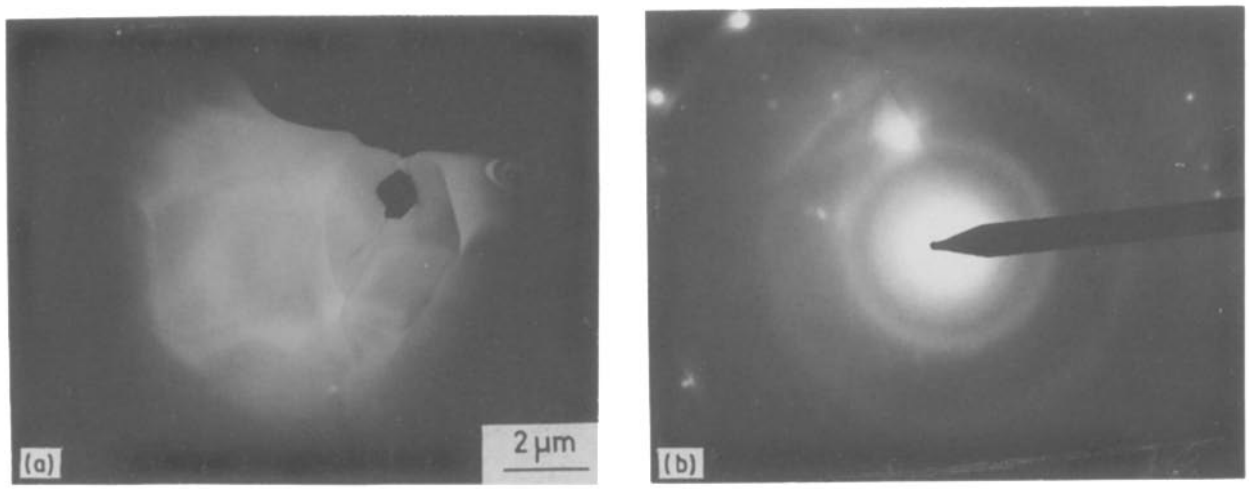

Figure 13 (a) CDF image of a glassy intergranular phase and (b) corresponding diffraction pattern. The circle represents the position of the objective aperture for obtaining microstructure (a).

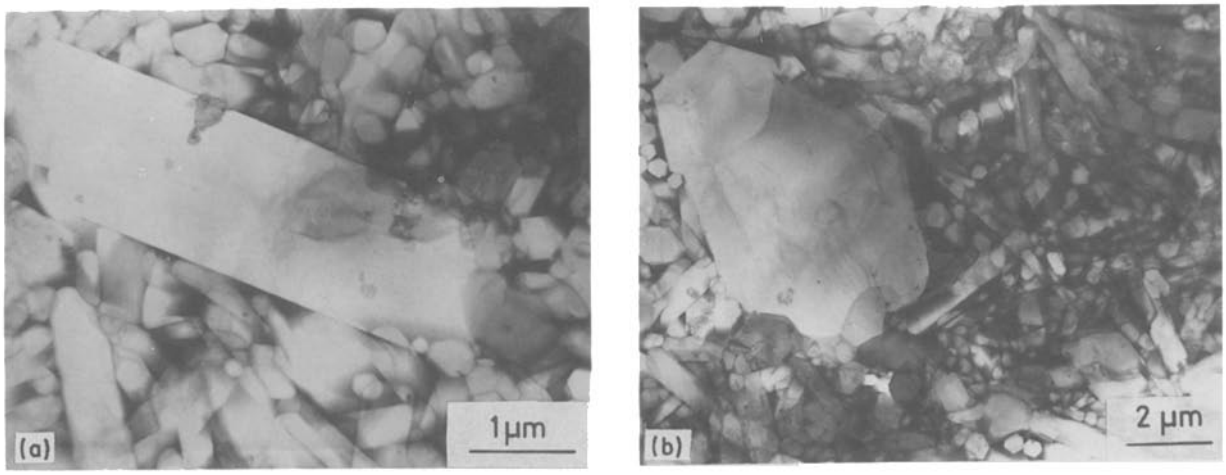

Figure 14 Transmission electron micrographs showing anomalously large grains suggesting (a) exaggerated β-grain growth, and (b) agglomeration.

penetration" has been identified [25] as a relaxation mechanism which releases the stored energy of deformation through the annihilation of dislocations by the sweeping action of the boundary, and is similar to the process of strain-induced boundary migration (SIBM) first reported in metallic systems [26, 27]. Although the energetics of these two processes (grain penetration and strain-induced boundary migration) is based upon similar concepts, the main distinction between them is that, whereas the bulging of the boundary in SIBM takes place by the atomic jumps across the boundary, in grain penetration there is always a thin layer of liquid in between the two grains. In the latter case, therefore, the movement of material may occur by different mechanisms which could actually involve diffusion through the liquid (e.g. solution–diffusion–precipitation). The energy balance is, however, favourable for this to occur because the substitution of distorted material by a dislocation-free crystal produces a decrease in the stored energy of the system.

In contrast to the microstructure observed for specimens containing a low ratio of Y_2O_3/Al_2O_3 as part of their chemical composition, second crystalline phases were observed for specimens containing none or only small amounts of alumina. Transmission electron micrographs showed, for instance (Fig. 16a), that a large proportion of the intergranular phase present in the specimen was crystalline, although a glassy phase of "similar" composition (see Fig. 16c and compare with Fig. 12b) coexisted with it. The crystalline second phase was generally observed at sites lying between β-Si_3N_4 grains, as clearly shown in Fig. 16 by the BF and CDF images. However, a thin film of a glassy phase (as that shown in Fig. 13) was observed between the β-grains and this crystalline intergranular phase. In fact the crystalline phase was never observed in between two β-grains if their separation was small. In those areas only the glassy phase was found to exist (Fig. 17a). Fig. 17b shows a further confirmation to this observation by noticing the direct lattice imaging effect of the β-Si_3N_4 grain and the amorphous character of its surroundings.

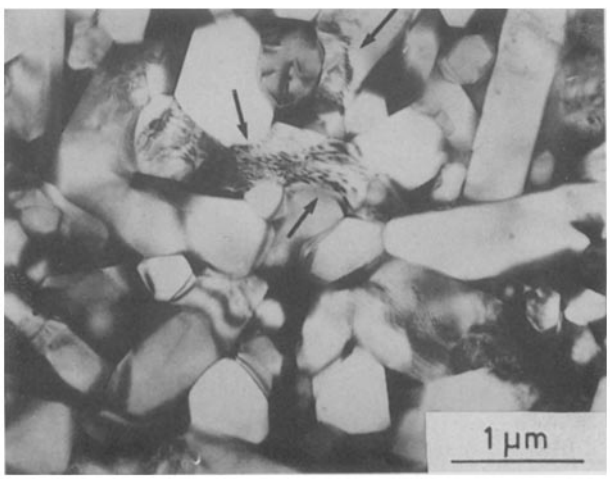

Figure 15 Transmission electron micrograph of a specimen of Si_3N_4 containing 6 wt % Y_2O_3 + 6 wt % Al_2O_3 sintered at 1750° C for 60 min under an argon pressure of 50 MPa.

4. Conclusions

This investigation indicates that sintering of silicon nitride at low pressures ($\simeq$ 0.5 MPa) only leads to high density when simultaneous additions of Y_2O_3 and Al_2O_3 are used. For a fixed amount of yttria added (3 or 6 wt % in the present work) a maximum in density (in percentage theoretical, %TD) can only be reached when an optimum amount of alumina is added. Additions in excess of this optimum will lead to a decrease of %TD. It was also observed that increasing the sintering temperature produced this maximum at higher densities and shifted its position towards lower concentrations of alumina. On the other hand, the results obtained indicate that sinter–HIP of Si_3N_4 with only small additions of Y_2O_3 and Al_2O_3 (less than 9 wt % in total) can lead to full density at temperatures around 1800° C and pressures below 50 MPa.

In this material it was observed that the α–β transformation kinetics is much faster than that of densification. The amount of β-phase found in each specimen strongly depended on composition and temperature. The influence of pressure on the transformation was observed to have an important effect after sinter–HIP of Si_3N_4 with no additions.

TEM work revealed that the microstructures of the analysed specimens consisted of elongated β-Si_3N_4 grains, with a mean grain size of about 1.5 μm, sur-

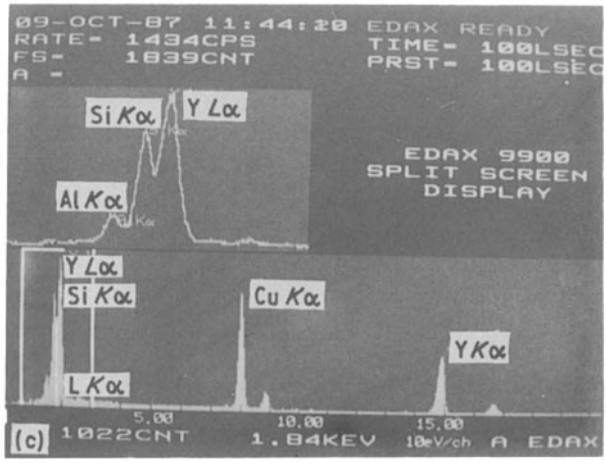

Figure 16 (a) BF and (b) CDF images of a crystalline intergranular phase in a Si_3N_4 + 20 wt % Y_2O_3 + 2 wt % Al_2O_3 specimen after sintering at 1800° C for 4 h in nitrogen. An EDS analysis obtained from that area is given (c).

rounded by an intergranular phase whose crystalline or amorphous state depended on the amount of alumina added to the basic Si_3N_4 + Y_2O_3 composition. It was clear that the crystallinity of the intergranular phase disappeared as the Y_2O_3/Al_2O_3 ratio decreased. A crystalline intergranular phase was only observed in alumina-free specimens and particularly in an Si_3N_4 + 20 wt % Y_2O_3 + 2 wt % Al_2O_3 specimen sintered at 1800° C for 4 h and cooled slowly. Also, even in the cases where the intergranular phase was found to be crystalline, an additional glassy phase was always present, mainly as a thin film ($\leqslant$ 0.5 to 2 nm) surrounding the β-Si_3N_4 grains and the crystalline intergranular phase itself. An important microstructural feature, produced by the application of pressure during sinter–HIP was observed in a specimen sintered at 1750° C under an argon pressure of 50 MPa. This is referred to as "grain penetration", takes place at some "contact points" between β-Si_3N_4 grains and is based on the elimination of the dislocations generated around the contact area, because of the application of high pressure.

Acknowledgement

The authors acknowledge Polmetasa and Departamento de Economía de la Diputación Foral de Guipúzcoa for the financial support provided to undertake this work.

References

1. G. R. TERWILLIGER and F. F. LANGE, *J. Amer. Ceram. Soc.* **57** (1974) 25.
2. *Idem, J. Mater. Sci.* **10** (1975) 1169.
3. R. E. LOEHMAN and D. J. ROWCLIFFE, *J. Amer. Ceram. Soc.* **63** (1980) 144.
4. L. J. BOWEN, T. G. CARRUTHERS and R. J. BROOK, *ibid.* **61** (1978) 335.

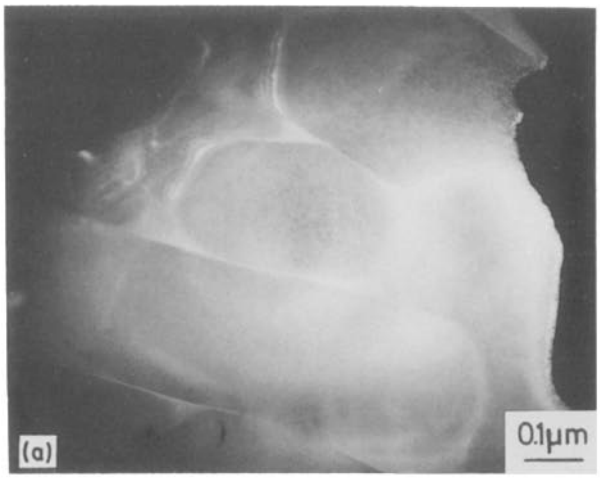

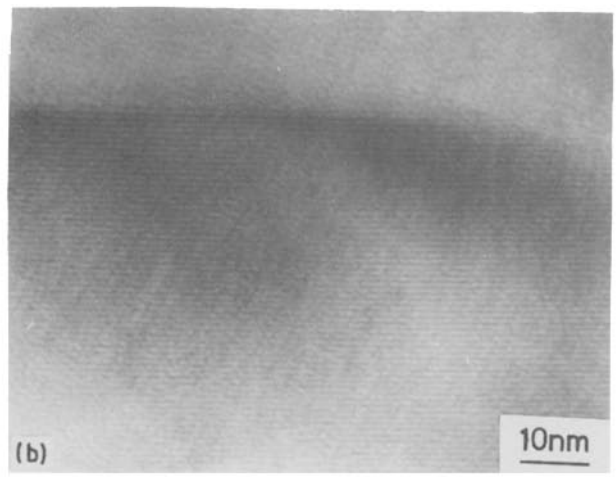

Figure 17 (a) CDF image of the vitreous intergranular phase and (b) direct lattice image of a β-silicon nitride grain.

5. J. GRESKOVICH and J. H. ROSOLOWSKI, *ibid.* **59** (1976) 336.
6. M. SHIMADA, A. TANAKA, T. YAMADA and M. KOIZUMI, in "Ceramic Powder", edited by P. Vincenzini (Elsevier Scientific, Amsterdam, 1983) pp. 871–9.
7. P. POPPER, in Proceedings of the International Symposium on Factors of Densification and Sintering of Oxide and Non-Oxide Ceramics, Japan 1978, edited by S. Soniya and S. Saito, pp. 19–27.
8. S. HAMPSHIRE and K. H. JACK, in "Special Ceramics 7" Proceedings of the British Ceramic Society, edited by D. Taylor and P. Popper, December, 1980 (British Ceramic Society, Stoke on Trent, 1981) pp. 37–49.
9. W. D. KINGERY and M. J. BERG, *J. Appl. Phys.* **26** (1955) 1205.
10. K. UENO and Y. TOIBANA, NASA Technical Memorandum, NASA TM-77424, Washington (1984).
11. R. R. WILLS, S. HOLINQUIST, J. M. WIMMER and J. A. CUNNINGHAM, *J. Mater. Sci.* **11** (1976) 1305.
12. G. WOTTING and G. ZIEGLER, in "Ceramic Powder", edited by P. Vincenzini (Elsevier Scientific, Amsterdam, 1983) pp. 951–62.
13. J. T. SMITH and C. L. QUACKENBUSH, in Proceedings of the International Symposium on Factors of Densification and Sintering of Oxide and Non-oxide Ceramics, Japan, 1978, pp. 426–42.
14. C. GRESKOVICH and C. PROCHAZKA, *J. Amer. Ceram. Soc.* **60** (1977) 471.
15. H. C. YEH and P. F. SIKORA, *Amer. Ceram. Soc. Bull.* **58** (1979) 444.
16. O. YEHESKEL, Y. GEFEN and M. J. TALIANKER, *J. Mater. Sci.* **19** (1984) 745.
17. C. GRESKOVICH, *J. Amer. Ceram. Soc.* **64** (1981) 725.
18. B. D. CULLITY, "Elements of X-ray Diffraction", 2nd Edn (Addison-Wesley, Mass., 1978).
19. G. E. GAZZA, *Amer. Ceram. Soc. Bull.* **54** (1975) 778.
20. A. ARIAS, *J. Mater. Sci.* **16** (1981) 787.
21. F. F. LANGE, *Int. Met. Rev.* **1** (1980) 1.
22. O. YEHESKEL, Y. GEFEN and M. TALIANKER, *J. Mater. Sci. Engng* **78** (1986) 209.
23. P. DREW and M. H. LEWIS, *J. Mater. Sci.* **9** (1974) 261.
24. G. ZIEGLER, J. HEINRICH and G. WOTTING, *J. Mater. Sci.* **22** (1987) 3041.
25. I. ITURRIZA, J. ECHEBERRÍA and F. CASTRO, in "Proceedings of the International Conference on Hot Isostatic Pressing of Materials: Applications and Developments", Antwerp, Belgium, April, 1988, to be published.
26. R. W. K. HONEYCOMBE, "The Plastic Deformation of Metals" (Arnold, London, 1968) Ch. 10.
27. J. W. MARTIN and R. D. DOHERTY, "Stability of Microstructure in Metallic Systems", Cambridge solid state science series (Cambridge University Press, 1976) Ch. 3.

Received 8 April
and accepted 7 September 1988